ACS Sustainable Chemistry & Engineering

pubs.acs.org/journal/ascecg

Research Article

Enhancement of Electricity Production of Microbial Fuel Cells by Using DNA Nanostructures as Electron Mediator Carriers

Shuo Han,[#] Krishna Thapa,[#] Wenyan Liu, David Westenberg, and Risheng Wang*

Cite This: *ACS Sustainable Chem. Eng.* 2022, 10, 16189−16196

Read Online

ACCESS | Metrics & More | Article Recommendations | Supporting Information

ABSTRACT: Microbial fuel cells (MFCs) are recognized as eco-friendly technology to convert chemical energy from waste into electricity by biocatalytic microorganisms and biomass as fuel feedstocks. Here, a three-dimensional DNA origami nanostructure serving as electron mediator-methylene blue (MB) carriers was first employed to enhance the electron production and transfer in the anode compartment of *Escherichia coli* system-based MFCs. By loading MB molecules on DNA origami nanostructures, the MFC with the MB/DNA origami-modified carbon felt (CF) electrode showed the highest voltage production (64 mV) and power density (5.78 mW/m^2) compared to bare CF and MB-modified CF electrodes. The enhanced MFC performance was attributed to the larger interface area of DNA origami-assisted MB loading and a biocompatible bacterial growth environment on the anode, which led to *E. coli* adhesion and fast electron transfer. Furthermore, the MFC with MB/DNA origami modifications could stably operate for three cycles (20 days) with constant voltage discharge without further addition of media. These results show that DNA origami is a promising material serving as an electron mediator carrier for sustainable energy systems, which could get over the drawbacks of carrier-free MFCs, such as short lifetime, continuously adding supplies, and toxicity to both the microorganisms and the natural environment.

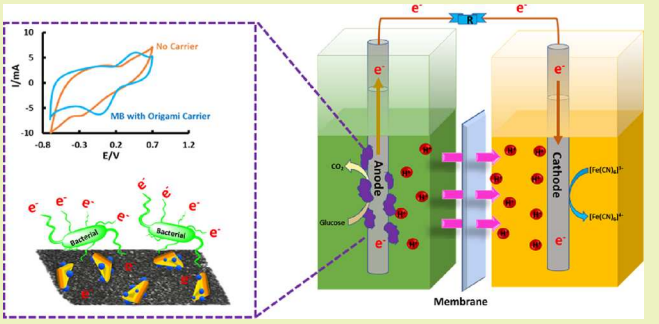

KEYWORDS: *microbial fuel cells, DNA origami, electron mediator, methylene blue, E. coli*

INTRODUCTION

Microbial fuel cells (MFCs) have emerged as a promising technology for wastewater treatment and an ultimate source of sustainable green energy in recent years.[1−3] MFCs are biological fuel cells that can generate electricity through the electrons produced during bacterial metabolism[4] via oxidizing a variety of substrates like acetate, glucose, etc.[5,6] Depending on the nature of the bacteria, those electrons are transported to the electrode either directly through membrane-bound redox-active proteins, such as *c*-type cytochromes and iron−sulfur proteins, and by electrically conductive protein filaments called "conductive nanowires" or in an indirect way using redox-active electron mediators, such as flavonoids and anthraquinones.[7−10] Although the direct electron transfer from microorganisms has some advantages, this process is not very effective in electron transfer kinetics and current generation. In contrast, the electron mediators promote electricity production in MFCs, increasing the viability and performance of the bio-electrochemical system.[11]

Generally, electron mediators are low molecular weight substances that undergo repeated redox reactions and shuttle electrons between the bacterial cells and the electrode. In recent years, various electron transfer media, such as neutral red, safranine O, methyl violet, methylene blue, thionine, humic acid, and anthraquinone-2,6-disulfonic acid, have been utilized to facilitate electrical current production from bacteria.[12−17] For example, Li and Zhou found that Cu(II) as an electron-shuttle mediator enhanced the electron transfer rate in MFCs, which showed a 1.44 times increase in power density and 1.17 times increase in reduction rate compared with the absence of Cu(II).[18] Sund et al. also studied the effects of electron mediators (9,10-anthraquinone-2,6-disulfonic acid disodium salt (AQDS), safranine O, resazurin, methylene blue, and humic acids) on current production from cellulose digestion by *Clostridium cellulolyticum* in MFCs.[19] It was shown that mediators have considerable enhancements on the current output of MFCs because the metabolism of the bacteria was increased significantly by those electron mediators. Even though the electron mediators show good ability to increase the current production in MFCs, the low solubility, high toxicity, and difficulty in accessing the bacterial

Received: July 23, 2022
Revised: November 10, 2022
Published: November 22, 2022

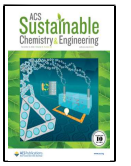

https://doi.org/10.1021/acssuschemeng.2c04399
ACS Sustainable Chem. Eng. 2022, 10, 16189−16196

Scheme 1. Schematic Illustration of the Design of an MFC Using MB/DNA Origami-Modified Carbon Felt as the Anode to Enhance the Electron Transfer

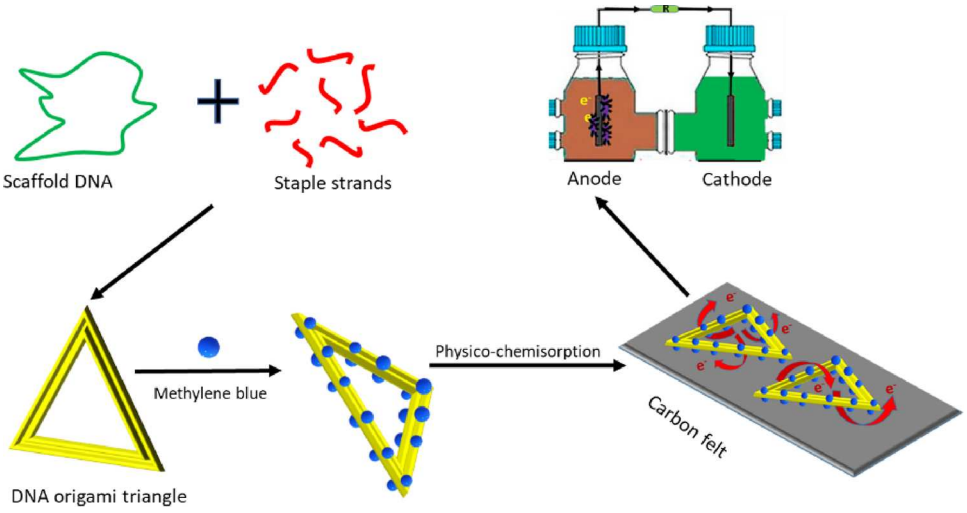

electron source are still significant bottlenecks in the practical application of MFCs.[20]

Methylene blue (MB) is an efficient mediator with good solubility and redox characteristics.[21−23] Popov et al. presented that MB exhibited good binding as a mediator molecule to the electrode surface and improved the performance of MFCs.[24] Daniel et al. found that MB produced a higher power output than neutral red when used in MFCs as a mediator.[25] Permana et al. investigated the performance of MFCs with and without MB as an electron mediator utilizing *Saccharomyces cerevisiae* as biocatalysts and glucose as a substrate to generate electricity.[26] Their study showed that the use of MB yielded higher cell potential. However, challenges still exist in the application of MB for MFCs, of particular concern, its low electron transfer efficiency, and biological incompatibility. Together, these factors seriously impede its application in large-scale MFC reactors. Therefore, to overcome these limitations, a high-efficiency electron carrier capable of providing an extensive interface for loading mediators and an uninterrupted supply of electrons released in the MFC over several days or weeks is highly desired.

With its ability to self-assemble into diverse multidimensional structures, DNA origami[27] has shown great promise as a carrier for small organic molecules, such as chemotherapy drugs and fluorescent dyes, because of their superior structural programmability and natural biocompatibility.[28−30] MB is positively charged in solution and shows great binding capability with DNA strands.[31,32] Importantly, the redox characteristic of MB is not affected by the association process between DNA and MB. Previous work has demonstrated that MB intercalated with DNA molecules can proceed with electron transfer rate constants varying from 10^5 to 10^{10} s^{-1} through the electronically coupled DNA base-pair π-stack.[33] DNA origami is constructed with multiple chains of DNA duplex providing more embedded positions for MB than in a single DNA duplex. Therefore, the complexes of the MB-DNA origami structure would have great potential to increase the electron transfer process and provide a biocompatible environment for bacteria. Here, we proposed a novel strategy that the employed MB/DNA nanostructure-modified carbon felt serves as the anode to enhance the electron transfer process and the subsequent electricity production in an "H"-type MFC (see Scheme 1). *Escherichia coli* was selected for this design as a well-characterized electrogenic bacterium with a high proliferation rate and can be adopted in an extreme environment.[34] In addition, *E. coli* has been reported to have good performance in MFCs using carbon felt as the anode but needs a mediator to enhance the electron transport efficiency.[35] The surface of the carbon felt anode was modified with MB-loaded 3D triangular-shaped DNA origami nanostructures[36] through electrostatic interaction, which dramatically increased the loading yield of MB on the anode surface, while the attachment of DNA origami on the surface of the anode provided a more biocompatible environment for the bacterial growth. On the porous structure of carbon felt, *E. coli* colonized, forming biofilms, generating electrons, and transporting electrons to high density MB during its metabolism. The performance of MFCs with MB and MB/DNA origami complex-treated electrodes was compared to measure the efficiency of DNA origami nanostructures as a mediator carrier to transfer electrons using cyclic voltammetry, power density, and voltage output capability. Compared with the MB alone-immobilized anode MFC, MB/DNA origami modification of the MFC shows better voltage generation and higher power density. Our results suggested that the 3D DNA origami carrier design was effective and might provide a useful strategy for improving MFC efficiency.

MATERIALS AND METHODS

Materials. DNA origami staple strands were purchased from Integrated DNA Technologies, Inc., were stored in 96-well plates with a concentration of 100 μM, and were used without further purification. Single-stranded M13mp18 viral DNA was purchased from Bayou Biolabs. Methylene blue (MB) was purchased from Sigma-Aldrich, Inc. The wild-type *E. coli* K-12 strain was used (Missouri S&T microbiology culture collection). The lysogeny broth (LB) medium used to culture the bacteria was purchased from Thermo Fisher Scientific, NJ, USA. The carbon felt (PEM, Nafion 117) was purchased from Fuel Cell Earth, MA., USA.

Methods. *DNA Origami Carrier Construction and the Loading of Methylene Blue.* DNA origami nanostructures were constructed by following a previous report.[27] Briefly, M13mp18 single-stranded viral DNA (20 nM) was mixed with synthesized staple strands at a molar ratio of 1:5 in a 1× TAE buffer with 11.5 mM Mg^{2+}. The mixture was annealed by slowly cooling from 90 to 16 °C in a period of 12 h in a thermocycler (Eppendorf). The DNA origami was then purified using

https://doi.org/10.1021/acssuschemeng.2c04399
ACS Sustainable Chem. Eng. 2022, 10, 16189−16196

100 kDa MWCO centrifugal filters purchased from Pall, Inc., to remove excess staple strands. The successful formation of the DNA origami nanostructures was studied with atomic force microscopy (AFM, Bruker Dimension Icon instrument). MB/DNA origami complexes were prepared by mixing DNA origami nanostructures (5.0 nM) and MB (100 μM) and then incubating at 37 °C for 24 h. After incubation, the mixture was centrifuged, and the supernatant containing free MB was removed. The supernatant collected was characterized by using a UV−visible spectrophotometer at an absorbance of 668 nm. The concentration of free MB in the supernatant was calculated based on an MB standard curve to justify the MB loading yield. The MB/origami precipitate was then resuspended in 1× PBS buffer with a total volume of 3 mL. The final concentrations of MB (20 μM) and DNA origami (3 nM) in MB/origami complexes were again determined by a UV-visible spectrophotometer. The prepared MB/DNA origami was stored at 4 °C.

"H"-MFC Electrode Modification and the Reactor Setup. The LB medium (25 mg/L) was prepared and used to grow bacteria following anaerobic techniques. The cultures were incubated in a 37 °C shaking incubator at 200 RPM overnight and subsequently transferred into a fresh growth medium. Once the log optical density (OD_{600}) was observed at 1.4 (see Figure S1), the cultures were inoculated into the MFC reactors in a 2:3 ratio with anode electrolytes (0.31 g/L NH_4Cl, 2.452 g/L NaH_2PO_4 H_2O, 4.576 g/L Na_2HPO_4, 0.13 g/L KCl, and 1 g/L $C_6H_{12}O_6H_2O$ at pH 7.0). The biofilm was formed on the electrode surface during the acclimatization period. After the growth, the medium was replaced with anolyte only. For MB-treated CF, the anode CF (2.0 cm × 3.0 cm) was immersed into 20 μM MB solution for 28 h and then dried for another 28 h.[24] The same procedure was repeated for MB/DNA origami modification treatment. To determine the stability of the redox properties of the MB/DNA origami-modified CF electrode, cyclic voltammetry (CV) was performed by cycling the potential of a working electrode up to 30 times and compared with bare CF (scan range: −0.7 to +0.7 V, at a scan rate of 5 mV/s in a 1× PBS buffer). As shown in Figure S2, asymmetric CV was obtained for bare CF with the reduction peak at −0.37 V. The current peaks were consistent within 30 scan cycles with slight increments in current value (Figure S2A). The MB/DNA origami-modified CF electrode exhibited similar stability with redox peaks at 0.15 and −0.37 V (Figure S2B), over 30 cycles. The effects of the MB concentration on the growth of *E. coli* were also studied (shown in Figure S3). It was found that the growth of bacteria with 20 μM MB is similar to the growth on the bare CF, demonstrating that 20 μM MB has a minor toxic effect on the bacterial growth. Therefore, in our MFC system, the concentration of MB was controlled at 20 μM. A double-chambered membrane MFC reactor was constructed with two glass bottles of 50 mL capacity joined with a glass bridge containing a proton exchange membrane (PEM). The PEM was pretreated before use in MFCs by heating (≈80 °C) in 3% H_2O_2 for an hour, followed by Milli-Q water for 2 h, and finally in 0.5 M H_2SO_4 for an hour, with the membrane being rinsed thoroughly after each step. The distance between the anode and cathode was 8 cm. The external circuit resistance was fixed at 1 KΩ. The cathodic compartment was filled with the analytes: 50 mM ferricyanide and 50 mM phosphate buffer solution (4.576 g/L Na_2HPO_4, 2.452 g/L $NaH_2PO_4{\cdot}H_2O$, and 0.13 g/L KCl).

Power Density and Cyclic Voltammetry Measurements. The cell density in culture solution was determined using a UV−visible spectroscopy system at a wavelength of 600 nm. The voltages generated by the MFCs during the experiments were recorded by a multimeter. Power density was calculated in eq 1 according to Logan et al.[37]

$$P = UI/S \quad (1)$$

$$I = U/R \quad (2)$$

The current (I) was calculated using Ohm's law (eq 2), where U is the voltage and R is the external resistance; the calculated current was divided by the surface area of the anode (S) and then multiplied by the voltage to obtain the power density based on eq 1, where P is the power density (mW/m^2). The Ag/AgCl electrode was used as a reference to measure the anode and cathode potentials. Cyclic voltammetry was performed using a potentiostat (IVUM soft, Ivium Technology, Eindhoven, the Netherlands) in a three-electrode system. The working electrode was connected to the counter electrode at a scan rate of 50 mV/s over the range of −700 to +700 mV (vs Ag/AgCl).

Scanning Electron Microscopy (SEM). After the experiment, the biofilm that adhered to the CF anode of the MFC was analyzed by SEM. Samples of the biofilm on the electrode (0.5 cm × 0.5 cm × 0.5 cm) were fixed by using 2.5% glutaraldehyde in PBS buffer (pH 6.8) for 1.5 h at 4 °C. After which, the samples were washed with PBS buffer three times (10 min each time). The samples were dehydrated in increasing concentrations (50, 70, 80, and 90%) of ethanol (10 min each time). At last, the samples were dehydrated with 100% ethanol three times (15 min each time) and dried for 12 h.[38] The electrode surface morphology was investigated with SEM (Hitachi S-4700). The sample was made conductive by coating with Au/Pd using a VENTOR coater with a sputtering current of 8 mAmp for 60 s. The 15 kV accelerating voltage was applied, and a standard secondary electron detector was used for surface imaging.

Biofilm Protein Assay. When the biofilm of *E. coli* was formed on the electrode surface (indicated by reaching the highest voltage in measurement of the MFC), the anode electrode was removed and ultrasonically treated in 15 mL of deionized water for 30 min. Water (1 mL) with biomass suspended in it was pipetted from ultrasonically treated solution and then subjected to centrifugation at 2000 rpm for 2 min. Afterward, 0.5 mL of the supernatant was mixed with 0.5 mL of 0.1 M NaOH solution. The mixture was boiled for 20 min in a water bath until the sample was clear. Finally, the biomass protein was determined by the modified Lowry method.[39]

RESULTS AND DISCUSSION

Construction of Nanoscale MB Carriers from DNA Origami. In this study, 3D triangular-shaped DNA origami nanostructures designed by Liu et al.[36] were employed as the MB carriers. The successful formation of DNA origami was studied with atomic force microscopy (AFM), as shown in Figure 1. The morphology of the structures is consistent with the design in a high yield, and the measured edge length of the triangle is ∼50 nm. To enhance the electron transfer efficiency, artificial mediators will be added to the system, which takes the responsibility to transport electrons from microbial cells to the surface of the electrode. Those molecules should be stable in

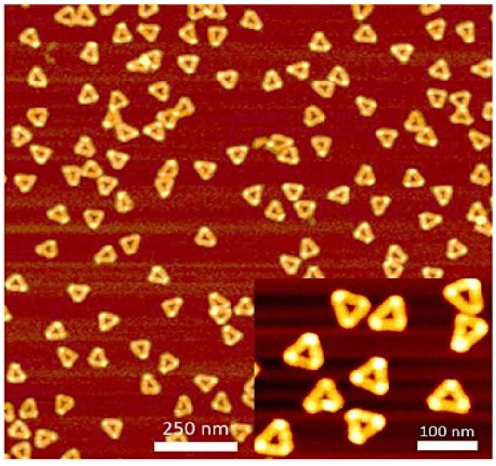

Figure 1. AFM image showing the formation of DNA origami triangles.

https://doi.org/10.1021/acssuschemeng.2c04399
ACS Sustainable Chem. Eng. 2022, 10, 16189−16196

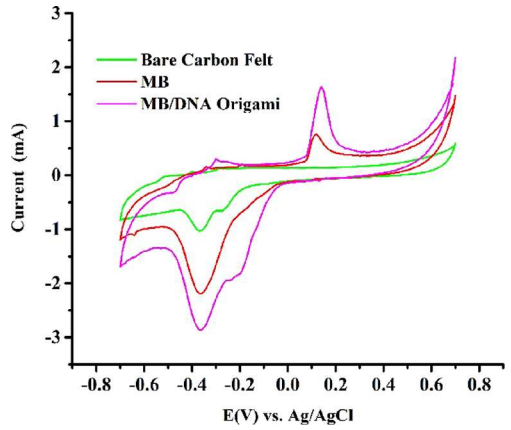

Figure 2. Cyclic voltammograms of different types of carbon felt electrodes. Bare electrode (green), MB-modified electrode (red), and MB/DNA origami-modified electrode (pink).

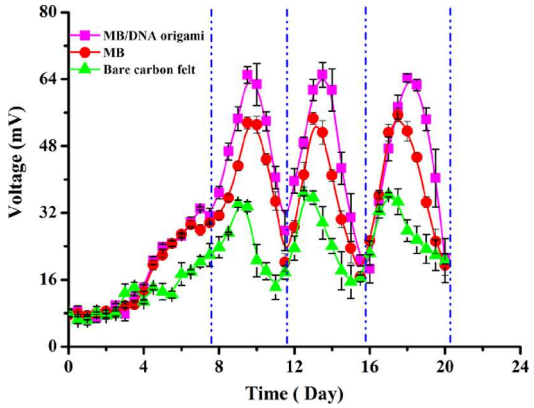

Figure 3. Development of voltages in MFCs with bare carbon felt and MB and MB/DNA origami-modified electrodes during the enrichment process.

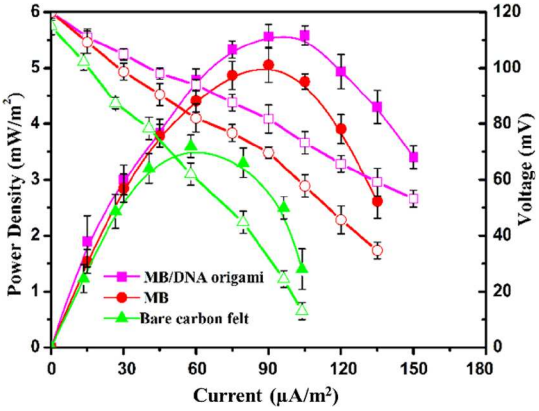

Figure 4. Comparison of power densities and polarization curves for MFCs with MB and MB/DNA origami-treated CF electrodes.

both oxidized and reduced forms and should not be toxic to the biological species at higher concentrations. However, common mediators contribute toxicity to the biological medium.[40] To overcome these drawbacks, DNA origami serves as MB carriers that not only increases the loading yield of MB but also provides a biocompatible environment for bacterial attachment and growth on the electrode surface. After the formation of DNA origami, the mixture of MB (100 μM) and DNA origami (5 nM) was incubated at 37 °C for 24 h. The loading efficiency was calculated by measuring the free MB before and after loading, which is ∼61.5% (Figure S4). In the AFM image, it was observed that the interaction of MB and DNA origami did not affect the morphology of nanostructures (Figure S5). The MB molecules associated with DNA origami were reduced by accepting electrons from microbial cells, then released the electrons to the electrode, and reoxidized thereafter. The redox reaction of MB is given in eq 3

$$MB_{(reduced)} \rightarrow MB_{(oxidized)} + 2e^- + H^+ \quad (3)$$

Physico-Chemisorption of MB onto the Carbon Electrode. Before introducing the DNA origami nanostructures into the system for MB mediator carriers, whether DNA nanostructures affect the bacterial growth, the charge transfer behavior between *E. coli* and the electrode or not was investigated first. The growth of bacteria was monitored in both the LB medium and the mixture of DNA origami (3 nM) and the LB medium. As shown in Figure S6A, it exhibits no toxicity to *E. coli*. In addition, the DNA origami alone-modified CF electrode was prepared. The CV curve (Figure S6B) shows a similar trend as the bare CF. It means that DNA origami did not have significant effects on the electrochemical characteristics of CF electrodes and does not affect their charge transfer behavior, which recommends the DNA nanostructures' prospective application in the MFC and related fields.

To investigate physico-chemisorption of MB onto the CF electrode, CV tests were conducted. CV of bare CF was compared with MB-modified CF and MB-loaded DNA origami (MB/DNA origami)-modified carbon felt. Figure 2 shows that the reduction and oxidation peaks with increased current amplitude were obtained from the MB/DNA origami-treated CF electrode (1.6 mA at 0.14 V and −2.8 mA at −0.36 V, respectively) compared to MB-treated electrodes (0.8 mA at 0.12 V and −2.2 mA at −0.36 V, respectively) and bare electrodes (no oxidation peak, −1.02 mA at −0.36 V for reduction). It is known that MB can interact with DNA by electrostatic interaction, MB-DNA intercalation, and π-stacking insertions[41] without affecting the conformation of 3D DNA origami triangles. The increase in current by almost 2-fold in oxidation and 3-fold in reduction with MB/DNA origami modification compared to the MB-modified electrode could be attributed to the larger DNA nanostructure interfaces that increase the amount of MB strongly bonded on the electrode surface. As a control, MB-loaded dsDNA (1 μM) (MB/dsDNA) was also used to modify the CF electrode. As shown in Figure S7, the oxidation peak of MB/dsDNA is slightly higher than the MB-treated electrode and much lower than MB/DNA origami, although they contain a similar amount of deoxyribonucleotides. These results suggest that the 3D DNA origami nanostructures serving as the MB carrier could greatly enhance MB loading and electron transfer efficiency.

Performance of MB/DNA Origami as Mediator Carriers in MFC. *Voltage Generation.* In this study, the MFC utilizes the glucose decomposition by *E. coli* to produce energy currency. Glucose taken into the microbial cells is oxidized and decomposed by various enzymes via an intercellular glycolysis system to produce electrons and protons in the anode chamber of the MFC, where the electrons released will be transferred to the anode via an MB mediator, acting as an electron shuttle, and protons travel to the cathode chamber via a proton exchange membrane. The produced

https://doi.org/10.1021/acssuschemeng.2c04399
ACS Sustainable Chem. Eng. 2022, 10, 16189−16196

Table 1. Comparison of the MFC Performances with Reported Systems

stains	method/technique	electrode	power density	ref
Shewanella sp.	methylene blue (10 mM)	graphite carbon cloth	14.06 mW/m^2	44
E. coli	methylene blue (25 mM)	graphite carbon cloth	46.14 mW/m^2	44
E. coli	gene engineering	carbon paper	3.41 μW/cm^2	45
E. coli	gene engineering	gold-coated glass slides	0.27 mW/m^2	46
mixed microflora	methylene blue (1.34 mM)	carbon veil electrode	11.3 W/m^3	24
mixed microflora	neutral red (1.34 mM)	carbon veil electrode	3.1 W/m^3	24
E. coli	methylene blue (0.3 mM)	graphite carbon cloth	3.98 mW/m^2	47
S. cerevisiae	methylene blue (5 mM)	graphite rods	45 μW/cm^2	48
Pichia fermentans	methylene blue (1.5 μM)	carbon fiber	1.64 mW/cm^2	49
S. cerevisiae	methylene blue (5 mM)	copper electrode	4.48 mW/m^2	26
mixed microflora	methylene blue (100 μM)	graphite rod	337.13 mW/m^3	26
S. cerevisiae	methylene blue (300 μM)	graphite	12.3 μW	50
S. cerevisiae	methylene blue (0.1 mM)	carbon felt	429.29 mW/m^2	51
S. cerevisiae	methylene blue (20 μM)	carbon-fiber brush	5.2 W/m^3	52
E. coli	methylene blue in the 3D DNA origami carrier (20 μM)	carbon felt	5.78 mW/m^2	this study

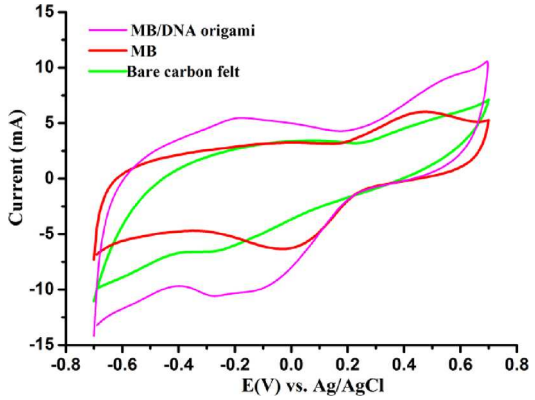

Figure 5. Cyclic voltammetry curves of MFCs with MB, MB/DNA origami-modified electrodes, and bare carbon felt control during the steady state of electricity generation.

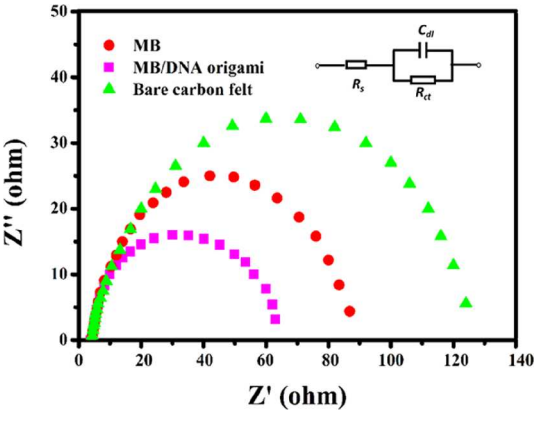

Figure 6. Electrochemical impedance spectroscopy of the MFC with MB, MB/DNA origami-modified electrodes, and bare carbon felt control during the steady state of electricity generation (inset: the equivalent circuit).

electrons from the anode will go through an external circuit, as shown in Scheme 1, and consequently enter the cathode, where the reduction reaction takes place. In the cathode chamber, ferricyanide is used for the electron acceptors because it has a high mass transfer efficiency and a high cathode potential so that a high output can be obtained.[42] It could be observed that the yellow color of $Fe[(CN)_6]^{3-}$ changed to yellow-green of $Fe[(CN)_6]^{4-}$ during the progress of the reduction in the cathode chamber. The potential differences between the two chambers produce voltage and current that generate bioelectricity. The reactions that occurred in the anode and cathode chambers of the MFC are described by the following equations:

$$\text{anode: } C_6H_{12}O_6 + 6H_2O \rightarrow 6CO_2 + 24H^+ + 24e^- \quad (4)$$

$$\text{cathode: } Fe[(CN)_6]^{3-} + e^- \rightarrow Fe[(CN)_6]^{4-} \quad (5)$$

Voltage generation in MFC chambers increased noticeably after 7 days following *E. coli* inoculation for all types of electrodes. MFCs with the MB/DNA origami-modified anode showed the most prominent increase in voltage output over time. As shown in Figure 3, the highest voltage of 64 mV was achieved with the MB/DNA origami-treaded anode, which was stable for 2 days. The MB-treated carbon electrode showed a relatively lower voltage, staying around 53.4 mV. The data indicates that the voltage output was increased by about 21% for MB/DNA origami compared to MB-treated anodes. The bare carbon felt showed a lag phase of 8 days, and then, the voltage increased to a maximum of 37.8 mV, lower than other MFCs. In addition, the maximum voltage output of the MB/dsDNA-modified MFC is around 52−55 mV (Figure S8), which is almost the same as the MB-MFC voltage output in Figure 3, while the voltage output of the pure DNA origami-modified MFC is similar to the bare CF (Figure S8). These results indicate that DNA origami not only served as MB carriers, which do not influence the reaction on the surface of electrodes, but also facilitated greater voltage output in the MFC due to the increase in the interfacial area of MB loading that enhances the electron transfer from bacteria to the electrode surface.

To confirm that the electricity production was mainly contributed by the biofilm, CV under both turnover and non-turnover conditions was recorded (scan rate: 1 mV/s, scan range: −0.7 V to +0.7 V) with a three-electrode system containing a working electrode as the anode, Ag/AgCl as the reference electrode, and a counter electrode as the cathode (Figure S9). To obtain the non-turnover conditions, when the voltage of the MFC decreased down to 12 mV, the anolyte was completely replaced with a fresh medium without glucose. The bacterial cytochromes present in the outer membrane could be responsible for redox peaks observed under non-turnover

https://doi.org/10.1021/acssuschemeng.2c04399
ACS Sustainable Chem. Eng. 2022, 10, 16189−16196

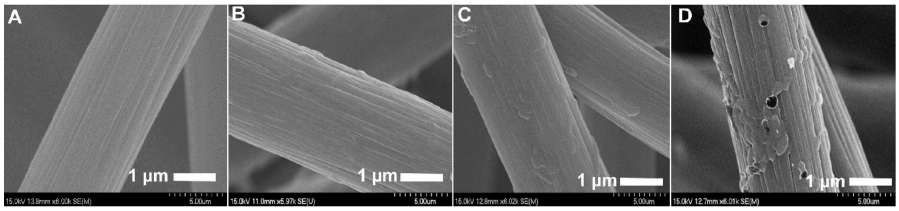

Figure 7. SEM images of carbon felt electrodes: (A) Bare carbon felt before using in the MFC. (B) Without modification in the MFC (control). (C) With absorption of MB in the MFC. (D) After absorption of MB/DNA origami in the MFC.

Table 2. Protein Assay for Three Types of Carbon Felt Electrodes

electrode	maximum voltage (mV)	maximum power densities (mW/m^2)	biomass (μg)
unmodified	37.8 ± 0.6	3.75 ± 0.20	235.35 ± 4.21
MB-modified	53.4 ± 1.4	4.82 ± 0.31	259.93 ± 3.42
MB/DNA-modified	64.0 ± 2.9	5.78 ± 0.21	284.51 ± 3.95

conditions.[43] The turnover CV curves exhibited higher redox peaks (at −0.24 and 0.27 V) corresponding to electrocatalytic activity toward glucose oxidation. Moreover, higher redox peaks for the MB/DNA origami-modified anode compared to bare CF provide insights that DNA origami assists in extracellular electron transfer in anodic biofilms.

Power Density. The polarization curve is obtained with different external resistances for the determination of maximum power and current under open-circuit conditions, which is an important analyzing tool to show the performance of the MFC. The voltage−current response was investigated to compare the maximum power density for MB and MB/DNA origami-treated carbon anodes as well as the bare carbon felt (Figure 4). The MB/DNA origami-treated anode consistently performed more effectively than the other two. The maximum power density reached 5.78 mW/m^2 for the MB/DNA origami-treated anode at a current density of 105 $\mu A/m^2$, while the power densities for MB and the bare carbon electrode were 4.82 mW/m^2 (90 $\mu A/m^2$) and 3.75 mW/m^2 (60 $\mu A/m^2$), respectively. The higher power density could be explained by the lower internal resistance in the MFC and the enhanced rate of electron transport facilitated by 3D MB/DNA origami complexes. The maximum power density of the designed MB/DNA nanocomposite was subsequently compared with literature work, taking into account parameters such as microorganisms, mediators' concentration, and MFC electrodes (Table 1). Results summarized in Table 1 demonstrate the potential of the proposed 3D MB/DNA origami modification of CF, showing comparable performance to recent similar work.

Cyclic Voltammetry (CV) and Electrochemical Impedance Spectroscopy (EIS). Cyclic voltammetry (CV) was used to investigate the redox activities of modified carbon felt electrodes in MFCs. The CV plots of the anodic medium after running the MFC with different electrodes at a scan rate of 50 mV/s are shown in Figure 5. The oxidation and reduction peaks are more significant for MB/DNA origami-treated electrodes than others. The current increase was because of the higher electrochemical redox activities created by biocompatible DNA origami as the MB carrier, indicating that the 3D MB/DNA origami complexes had more effects on increasing the redox activities of the MFC. These results demonstrate that the electrons produced during bacterial metabolism were successfully carried out by redox-active MB/DNA origami complexes to the electrode surface, assisting in extracellular electron transfer. The lower activity of MB-treated MFCs might be because of the toxicity of MB, decreasing bacterial growth and subsequently their metabolism.

EIS is a useful technique to observe the bioelectrochemical phenomenon occurring in the MFC, which has been extensively utilized to determine the internal resistance (R_{in}) of the MFC. EIS tests were subsequently conducted in the two-chamber H-type MFC. The Ag/AgCl reference electrode was located adjacent to the working electrode in the anode compartment, and the cathode electrode played the role as a counter electrode. Based on the Nyquist plots and equivalent circuit (Figure 6), the R_{in} is mainly generated by solution resistance (R_s) and charge transfer resistance (R_{ct}). The charge transfer resistance of the control MFC system with bare CF was 125 Ω. Resistance for the MB/DNA origami MFC was 62 Ω, indicating that MB/DNA modification on the anode surface resulted in a higher rate of electron transfer at the bioanode−electrolyte interface, which may prompt higher biocatalytic activity of the anode and more electrons transfer to the cathode, and hence enhanced bioelectricity generation.

Scanning Electron Microscopy. To confirm the formation of *E. coli* biofilms on the surface of the carbon felt electrodes, SEM images were collected (shown in Figure 7 and Figure S10). SEM images showed variations in bacteria attached to the anode surfaces depending on their surface properties. Only a few bacteria were grown on the bare carbon felt and MB-treated electrode surfaces. In contrast, the MB/DNA origami-treated electrode surface is beneficial to more bacterial attachments, demonstrating that the treatment of carbon felt with MB/DNA origami increased surface roughness, providing a biocompatible environment assisting in biofilm growth.

Protein Assay. The modified Lowry method[39] was followed to measure the total amount of biofilm growth on three different electrodes. The calibration curve with the standard protein assay is given in the Supporting Information (Figure S11). The highest amounts of biofilm were found on the MB/DNA origami-modified carbon felt anode (284.51 μg) and MB-modified carbon felt electrode with 259.93 μg and least on the control carbon felt electrode with 235.35 μg (Table 2).

CONCLUSIONS

In summary, we investigated a novel method to enhance the electron transfer between the electrode and bacteria by using 3D DNA origami as electron mediator carriers in MFCs. Our results demonstrated the increase in the electricity production by using the MB/DNA origami-modified carbon felt electrode over the MB-modified electrode because DNA origami exhibited enhanced bioelectrical capabilities with larger

https://doi.org/10.1021/acssuschemeng.2c04399
ACS Sustainable Chem. Eng. 2022, 10, 16189−16196

interface reaction areas and a biocompatible bacterial growth environment compared to MB molecules. The power densities of MFCs with DNA carriers can be ~36 and ~17% higher at the MFC's highest and stable voltage, compared to the power densities obtained from the MB-modified electrode and bare carbon felt, respectively. Moreover, this study provides a new and promising strategy to apply DNA nanostructures in the ecosystem.

■ ASSOCIATED CONTENT

Supporting Information

The Supporting Information is available free of charge at https://pubs.acs.org/doi/10.1021/acssuschemeng.2c04399.

Growth curve of *E. coli*, stability test of CF electrodes, AFM images of DNA nanostructures, SEM images of CF electrodes, cyclic voltammograms of modified electrodes, and DNA sequences (PDF)

■ AUTHOR INFORMATION

Corresponding Author

Risheng Wang − *Department of Chemistry, Missouri University of Science and Technology, Rolla, Missouri 65409, United States;* orcid.org/0000-0001-6539-1565; Email: wangri@mst.edu

Authors

Shuo Han − *Department of Chemistry, Missouri University of Science and Technology, Rolla, Missouri 65409, United States*

Krishna Thapa − *Department of Chemistry, Missouri University of Science and Technology, Rolla, Missouri 65409, United States*

Wenyan Liu − *Department of Chemistry, Missouri University of Science and Technology, Rolla, Missouri 65409, United States; Center for Research in Energy and Environment, Missouri University of Science and Technology, Rolla, Missouri 65409, United States*

David Westenberg − *Department of Biological Sciences, Missouri University of Science and Technology, Rolla, Missouri 65409, United States*

Complete contact information is available at: https://pubs.acs.org/10.1021/acssuschemeng.2c04399

Author Contributions

#S.H. and K.T. authors contributed equally.

Notes

The authors declare no competing financial interest.

■ ACKNOWLEDGMENTS

This work was supported by the National Science Foundation under grant CCF-1814797 and Office of Research, Missouri University of Science and Technology.

■ REFERENCES

(1) Obileke, K.; Onyeaka, H.; Meyer, E. L.; Nwokolo, N. Microbial fuel cells, a renewable energy technology for bio-electricity generation: A mini-review. *Electrochem. Commun.* **2021**, *125*, 107003.

(2) Liu, W. F.; Cheng, S. A. Microbial fuel cells for energy production from wastewaters: the way toward practical application. *J. Zhejiang Univ., Sci., A* **2014**, *15*, 841−861.

(3) Chaturvedi, V.; Verma, P. Microbial fuel cell: a green approach for the utilization of waste for the generation of bioelectricity. *BioResources Bioprocess.* **2016**, *3*, 1−14.

(4) Umar, M. F.; Abbas, S. Z.; Mohamad Ibrahim, M. N.; Ismail, N.; Rafatullah, M. Insights into Advancements and Electrons Transfer Mechanisms of Electrogens in Benthic Microbial Fuel Cells. *Membranes* **2020**, *10*, 205.

(5) Kondaveeti, S.; Mohanakrishna, G.; Pagolu, R.; Kim, I. W.; Kalia, V. C.; Lee, J. K. Bioelectrogenesis from Raw Algal Biomass Through Microbial Fuel Cells: Effect of Acetate as Co-substrate. *Indian J. Microbiol.* **2019**, *59*, 22−26.

(6) Dessi, P.; Chatterjee, P.; Mills, S.; Kokko, M.; Lakaniemi, A. M.; Collins, G.; Lens, P. N. L. Power production and microbial community composition in thermophilic acetate-fed up-flow and flow-through microbial fuel cells. *Bioresour. Technol.* **2019**, *294*, 122115.

(7) Aiyer, K. S. How does electron transfer occur in microbial fuel cells? *World J. Microbiol. Biotechnol.* **2020**, *36*, 19.

(8) Choi, O.; Sang, B. I. Extracellular electron transfer from cathode to microbes: application for biofuel production. *Biotechnol. Biofuels* **2016**, *9*, 11.

(9) Martinez, C. M.; Alvarez, L. H. Application of redox mediators in bioelectrochemical systems. *Biotechnol. Adv.* **2018**, *36*, 1412−1423.

(10) Li, T.; Yang, X.-L.; Chen, Q.-L.; Song, H.-L.; He, Z.; Yang, Y.-L. Enhanced Performance of Microbial Fuel Cells with Electron Mediators from Anthraquinone/Polyphenol-Abundant Herbal Plants. *ACS Sustainable Chem. Eng.* **2020**, *8*, 11263−11275.

(11) Kumar, A.; Hsu, L. H.-H.; Kavanagh, P.; Barrière, F.; Lens, P. N. L.; Lapinsonnière, L.; Lienhard, V. J. H.; Schröder, U.; Jiang, X.; Leech, D. The ins and outs of microorganism−electrode electron transfer reactions. *Nat. Rev. Chem.* **2017**, 0024.

(12) Rahimnejad, M.; Najafpour, G. D.; Ghoreyshi, A. A.; Bakeri, G.; Talebnia, F.; Oh, S.-E. Investigation of different mediators in microbial fuel cell with cyclic voltammeter. *Pak. J. Biotechnol.* **2013**, *10*, 37−51.

(13) Rahimnejad, M.; Najafpour, G. D.; Ghoreyshi, A. A.; Talebnia, F.; Premier, G. C.; Bakeri, G.; Kim, J. R.; Oh, S. E. Thionine increases electricity generation from microbial fuel cell using Saccharomyces cerevisiae and exoelectrogenic mixed culture. *J. Microbiol.* **2012**, *50*, 575−580.

(14) Thygesen, A.; Poulsen, F. W.; Min, B.; Angelidaki, I.; Thomsen, A. B. The effect of different substrates and humic acid on power generation in microbial fuel cell operation. *Bioresour. Technol.* **2009**, *100*, 1186−1191.

(15) Logan, B. E.; Hamelers, B.; Rozendal, R.; Schröder, U.; Keller, J.; Freguia, S.; Aelterman, P.; Verstraete, W.; Rabaey, K. Microbial Fuel Cells: Methodology and Technology. *Environ. Sci. Technol.* **2006**, *40*, 5181−5192.

(16) Shana, O.; Kelley, J. K. B.; Jackson, N. M.; Hill, M. G. Electrochemistry of Methylene Blue Bound to a DNA-Modified Electrode. *Bioconjugate Chem.* **1997**, *8*, 31−37.

(17) Hao Pei, X.; Zhu, D.; Huang, Q.; Fan, C. Functional DNA Nanostructures for Theranostic Applications. *Acc. Chem. Res.* **2014**, *47*, 550−559.

(18) Li, M.; Zhou, S. Efficacy of Cu(II) as an electron-shuttle mediator for improved bioelectricity generation and Cr(VI) reduction in microbial fuel cells. *Bioresour. Technol.* **2019**, *273*, 122−129.

(19) Sund, C. J.; McMasters, S.; Crittenden, S. R.; Harrell, L. E.; Sumner, J. J. Effect of electron mediators on current generation and fermentation in a microbial fuel cell. *Appl. Microbiol. Biotechnol.* **2007**, *76*, 561−568.

(20) Lin, C.-W.; Wu, C.-H.; Chiu, Y.-H.; Tsai, S.-L. Effects of different mediators on electricity generation and microbial structure of a toluene powered microbial fuel cell. *Fuel* **2014**, *125*, 30−35.

(21) Han, T. H.; Khan, M. M.; Kalathil, S.; Lee, J.; Cho, M. H. Simultaneous Enhancement of Methylene Blue Degradation and Power Generation in a Microbial Fuel Cell by Gold Nanoparticles. *Ind. Eng. Chem. Res.* **2013**, *52*, 8174−8181.

(22) Huang, G.; Wang, H.; Zhao, H.; Wu, P.; Yan, Q. Application of polypyrrole modified cathode in bio-electro-Fenton coupled with microbial desalination cell (MDC) for enhanced degradation of methylene blue. *J. Power Sources* **2018**, *400*, 350−359.

(23) Khan, M. E.; Khan, M. M.; Min, B. K.; Cho, M. H. Microbial fuel cell assisted band gap narrowed TiO2 for visible light-induced photocatalytic activities and power generation. *Sci. Rep.* **2018**, *8*, 1723.
(24) Popov, A. L.; Kim, J. R.; Dinsdale, R. M.; Esteves, S. R.; Guwy, A. J.; Premier, G. C. The effect of physico-chemically immobilized methylene blue and neutral red on the anode of microbial fuel cell. *Biotechnol. Bioprocess Eng.* **2012**, *17*, 361−370.
(25) Daniel, D. K.; Das Mankidy, B.; Ambarish, K.; Manogari, R. Construction and operation of a microbial fuel cell for electricity generation from wastewater. *Int. J. Hydrogen Energy* **2009**, *34*, 7555−7560.
(26) Permana, D.; Rosdianti, D.; Ishmayana, S.; Rachman, S. D.; Putra, H. E.; Rahayuningwulan, D.; Hariyadi, H. R. Preliminary Investigation of Electricity Production Using Dual Chamber Microbial Fuel Cell (DCMFC) with Saccharomyces Cerevisiae as Biocatalyst and Methylene Blue as an Electron Mediator. *Procedia Chem.* **2015**, *17*, 36−43.
(27) Rothemund, P. W. Folding DNA to create nanoscale shapes and patterns. *Nature* **2006**, *440*, 297−302.
(28) Seeman, N. C. The design and engineering of nucleic acid nanoscale assemblies. *Curr. Opin. Struct. Biol.* **1996**, *6*, 519−526.
(29) Angell, C.; Xie, S.; Zhang, L.; Chen, Y. DNA Nanotechnology for Precise Control over Drug Delivery and Gene Therapy. *Small* **2016**, *12*, 1117−1132.
(30) Zeng, Y.; Liu, J.; Yang, S.; Liu, W.; Xu, L.; Wang, R. Time-lapse live cell imaging to monitor doxorubicin release from DNA origami nanostructures. *J. Mater. Chem. B* **2018**, *2018*, *6*.
(31) Ortiz, M.; Fragoso, A.; Ortiz, P. J.; O'Sullivan, C. K. Elucidation of the mechanism of single-stranded DNA interaction with methylene blue: A spectroscopic approach. *J. Photochem. Photobiol., A* **2011**, *218*, 26−32.
(32) Zhang, F. T.; Nie, J.; Zhang, D. W.; Chen, J. T.; Zhou, Y. L.; Zhang, X. X. Methylene blue as a G-quadruplex binding probe for label-free homogeneous electrochemical biosensing. *Anal. Chem.* **2014**, *86*, 9489−9495.
(33) Lewis, F. D.; Wasielewski, M. R.*Dynamics of photoinitiated hole and electron injection in duplex DNA*. Wiley Online Library: 2005, 93−116. DOI: 10.1002/3527606629.ch4
(34) Nguyen, D.; Taguchi, K. A disposable water-activated paper-based MFC using dry E. coli biofilm. *Biochem. Eng. J.* **2019**, *143*, 161−168.
(35) Nguyen, D. T.; Taguchi, K. Enhancing the performance of E. coli-powered MFCs by using porous 3D anodes based on coconut activated carbon. *Biochem. Eng. J.* **2019**, 151.
(36) Liu, W.; Li, L.; Yang, S.; Gao, J.; Wang, R. Self-Assembly of Heterogeneously Shaped Nanoparticles into Plasmonic Metamolecules on DNA Origami. *Chemistry* **2017**, *23*, 14177−14181.
(37) Logan, B.; Watsn, V.; Estadt, G. Graphite Fiber Brush Anodes for Increased Power Production in Air-Cathode Microbial Fuel Cells. *Environ. Sci. Technol.* **2007**, *41*, 3341−3346.
(38) Song, T.; Yang, C.; Zeng, G.; Yu, G.; Xu, C. Effect of surfactant on styrene removal from waste gas streams in biotrickling filters. *J. Chem. Technol. Biotechnol.* **2012**, *87*, 785−790.
(39) Wu, X. Y.; Tong, F.; Song, T. S.; Gao, X. Y.; Xie, J. J.; Zhou, C. C.; Zhang, L. X.; Wei, P. Effect of zeolite-coated anode on the performance of microbial fuel cells. *J. Chem. Technol. Biotechnol.* **2015**, *90*, 87−92.
(40) Velasquez-Orta, S. B.; Head, I. M.; Curtis, T. P.; Scott, K.; Lloyd, J. R.; Canstein, H. The effect of flavin electron shuttles in microbial fuel cells current production. *Appl. Microbiol. Biotechnol.* **2010**, *85*, 1373−1381.
(41) Farjami, E.; Clima, L.; Gothelf, K. V.; Ferapontova, E. E. DNA interactions with a Methylene Blue redox indicator depend on the DNA length and are sequence specific. *Analyst* **2010**, *135*, 1443−1448.
(42) Wu, C. H.; Lai, C. Y.; Lin, C. W.; Kao, M. H. Generation of power by microbial fuel cell with ferricyanide in biodegradation of benzene. *CLEAN−Soil, Air, Water* **2013**, *41*, 390−395.
(43) Marsili, E.; Rollefson, J. B.; Baron, D. B.; Hozalski, R. M.; Bond, D. R. Microbial biofilm voltammetry: direct electrochemical characterization of catalytic electrode-attached biofilms. *Appl. Environ. Microbiol.* **2008**, *74*, 7329−7337.
(44) Miroliaei, M.; Samimi, A.; Mohebbi-Kalhori, D.; Khorram, M.; Qasemi, A. Competition betweenE. coliandShewanella sp. for electricity generation in air cathode MFC in presence of methylene blue as artificial mediator. *Environ. Prog. Sustainable Energy* **2015**, *34*, 1097−1105.
(45) Nguyen, D.-T.; Tamura, T.; Tobe, R.; Mihara, H.; Taguchi, K. Microbial fuel cell performance improvement based on FliC-deficient *E. Coli strain*. *Energy Rep.* **2020**, *6*, 763−767.
(46) Jahnke, J. P.; Sarkes, D. A.; Liba, J. L.; Sumner, J. J.; Stratis-Cullum, D. N. Improved Microbial Fuel Cell Performance by Engineering E. coli for Enhanced Affinity to Gold. *Energies* **2021**, 14.
(47) Páez, A.; Lache-Muñoz, A.; Medina, S.; Zapata, J. Electric power production in a microbial fuel cell using Escherichia coli and Pseudomonas aeruginosa, synthetic wastewater as substrate, carbon cloth and graphite as electrodes, and methylene blue as mediator. Laboratory scale. *Tecnología y ciencias del agua* **2019**, *10*, 261−282.
(48) Rossi, R.; Setti, L. Effect of methylene blue on electron mediated microbial fuel cell by Saccharomyces cerevisiae. *Environ. Eng. Manage. J.* **2016**, *15*, 2011−2018.
(49) Pal, M.; Sharma, R. K. Exoelectrogenic response of Pichia fermentans influenced by mediator and reactor design. *J. Biosci. Bioeng.* **2019**, *127*, 714−720.
(50) Rahimnejad, M.; Najafpour, G. D.; Ghoreyshi, A. A.; Shakeri, M.; Zare, H. Methylene blue as electron promoters in microbial fuel cell. *Int. J. Hydrogen Energy* **2011**, *36*, 13335−13341.
(51) Christwardana, M.; Frattini, D.; Accardo, G.; Yoon, S. P.; Kwon, Y. Effects of methylene blue and methyl red mediators on performance of yeast based microbial fuel cells adopting polyethylenimine coated carbon felt as anode. *J. Power Sources* **2018**, *396*, 1−11.
(52) Yuan, J.; Liu, S.; Jia, L.; Ji, A.; Chatterjee, S. G. Co-Generation System of Bioethanol and Electricity with Microbial Fuel Cell Technology. *Energy Fuels* **2020**, *34*, 6414−6422.